

Autophagy, not apoptosis, plays a role in lumen formation of eccrine gland organoids

Lijie Du^{1,2}, Lei Zhang³, Junhong Zhao¹, Zixiu Chen¹, Xiang Liu¹, Manxiu Cao¹, Lei You⁴, Yonghong Zhang⁴, Xiaobing Fu⁵, Haihong Li^{1,2}

¹Department of Wound Repair and Dermatologic Surgery, Taihe Hospital, Hubei University of Medicine, Shiyan, Hubei 442000, China;

²Hubei Clinical Medical Research Center of Cord Blood Hematopoietic Stem Cells, Taihe Hospital, Hubei University of Medicine, Shiyan, Hubei 442000, China;

³Mental Health Center, Taihe Hospital, Hubei University of Medicine, Shiyan, Hubei 442000, China;

⁴School of Basic Medicine, Academy of Bio-Medicine Research, Hubei University of Medicine, Shiyan, Hubei 442000, China;

⁵Wound Healing and Cell Biology Laboratory, The First Affiliated Hospital, Chinese PLA General Hospital, Beijing 100048, China.

Abstract

Background: Sweat secreted by eccrine sweat glands is transported to the skin surface through the lumen. The eccrine sweat gland develops from the initial solid bud to the final gland structure with a lumen, but how the lumen is formed and the mechanism of lumen formation have not yet been fully elucidated. This study aimed to investigate the mechanism of lumen formation of eccrine gland organoids (EGOs).

Methods: Human eccrine sweat glands were isolated from the skin for tissue culture, and the primary cultured cells were collected and cultured in Matrigel for 14 days *in vitro*. EGOs at different development days were collected for hematoxylin and eosin (H&E) staining to observe morphological changes and for immunofluorescence staining of proliferation marker Ki67, cellular motility marker filamentous actin (F-actin), and autophagy marker LC3B. Western blotting was used to detect the expression of Ki67, F-actin, and LC3B. Moreover, apoptosis was detected using a terminal deoxynucleotidyl transferase dUTP nick end labeling (TUNEL) apoptosis assay kit, and the expression of poly (ADP-ribose) polymerase and Caspase-3 was detected by Western blot. In addition, 3-methyladenine (3MA) was used as an autophagy inhibitor to detect whether the formation of sweat glands can be effectively inhibited.

Results: The results showed that a single gland cell proliferated rapidly and formed EGOs on day 4. The earliest lumen formation was observed on day 6. From day 8 to day 14, the rate of lumen formation in EGOs increased significantly. The immunofluorescence and Western blot analyses showed that the expression of Ki67 gradually decreased with the increase in days, while the F-actin expression level did not change. Notably, the expression of autophagy marker LC3B was detected in the interior cells of EGOs as the apoptosis signal of EGOs was negative. Compared with the control group, the autophagy inhibitor 3MA can effectively limit the formation rate of the lumen and reduce the inner diameter of EGOs.

Conclusion: Using our model of eccrine gland 3D-reconstruction in Matrigel, we determined that autophagy rather than apoptosis plays a role in the lumen formation of EGOs.

Keywords: Eccrine sweat glands; Autophagy; Apoptosis; Lumen formation; Organoids

Introduction

Eccrine sweat glands are the most important skin appendages in humans and mammals. They are involved in a wide variety of important functions, such as body temperature regulation, secretion, and metabolism. Morphologically, the mature sweat glands are composed of a secretion portion found in the dermis and a duct that opens onto the surface of the skin.^[1] During the development of mouse embryo sweat buds, progenitors of sweat glands

form placodes on the epidermal basal layer and invaginate into the deep dermis. With further morphological changes of placodes, the cells at the tips of the sweat buds grow downward and differentiate into luminal cells and myoepithelial cells, forming the secretory coiled portion. The basal cells in the ducts extend upward and reach the skin surface, forming openings to connect the coil portion with the outer surface.^[2] Previous reports have shown that the other exocrine organs such as mammary glands and

Access this article online

Quick Response Code:



Website:
www.cmj.org

DOI:
10.1097/CM9.0000000000001936

Correspondence to: Haihong Li, Department of Wound Repair and Dermatologic Surgery, Taihe Hospital, Hubei University of Medicine, Hubei Clinical Medical Research Center of Cord Blood Hematopoietic Stem Cells, Taihe Hospital, Hubei University of Medicine, 32 South Renmin Road, Shiyan, Hubei 442000, China
E-Mail: lihaihong1051@126.com

Copyright © 2022 The Chinese Medical Association, produced by Wolters Kluwer, Inc. under the CC-BY-NC-ND license. This is an open access article distributed under the terms of the Creative Commons Attribution-Non Commercial-No Derivatives License 4.0 (CCBY-NC-ND), where it is permissible to download and share the work provided it is properly cited. The work cannot be changed in any way or used commercially without permission from the journal.

Chinese Medical Journal 2022;135(3)

Received: 14-07-2021; Online: 12-01-2022 Edited by: Ningning Wang

salivary glands mainly form cavities through cavitation, and some branched cells are likely to form lumens through the hollowing of cell bundles.^[3-5] In addition, sweat glands are one of the important exocrine glands for the transport of body fluids. The lumen formation mechanism of sweat glands has not been completely elucidated. Therefore, in-depth exploration of the progress of related luminal development has important research value.

The formation and functional reconstruction of three-dimensional (3D) organ morphology during development are the ultimate research goals of regenerative biology.^[6] Reconstruction in three dimensions is important for controlling and designing functional organs in potential medical applications, such as mammary, pancreatic, lacrimal, and salivary gland development and differentiation.^[7-10] These 3D-reconstitution systems are generated using strategies based on the common elements of cell behavior, including cell polarization, migration of tubular cells to target sites, diversification of cell fate, and positioning of specialized cells to different areas of the tubular system.^[6,11] A recent study used a 3D-reconstitution model by culturing Matrigel-embedded eccrine sweat gland cells (ESGCs) *in vitro* or by implanting them into the subcutis of nude mice and concluded that this model simulates the development, morphology, and function of sweat glands in natural form.^[12-16] Given that the tubular organs in the body have varying morphology, the tracking and analysis of lumen development in the body have become quite complicated, making us consider using this model to study the mechanism of lumen formation in sweat glands.

There are currently two main views of the mechanism mode of glandular lumen formation: cavitation (driven by cell death of inner cells) and cell bundle hollowing (driven by epithelial polarity without cell death).^[11] Cavitation means that in a multicellular cluster, adjacent unpolarized cells can recover apical-basal polarity, thereby creating a new cavity. As the plasma membrane and apical membrane separate, the cells in the central vacuole chamber undergo cell death as autophagy or apoptosis. When the products of cell death are gradually absorbed, the formation of the cell lumen is named cavitation. Autophagy and apoptosis usually involve the process of lumen formation through common forms of intraluminal cell death. For example, the formation of a mammary gland lumen during puberty occurs through the elimination of cells by apoptosis in newly branched epithelial bundles or newly formed acini, forming cavities. Cell bundle hollowing is directly established by membrane separation of polar epithelial cell clusters. In this mode, due to the coordination of cell division and polarization, an apical lumen can be formed between the two cells, without the involvement of hollow cell death.^[11] In addition, the actin cytoskeleton plays a central role in determining cell shape and polarity, providing structural support, and promoting cell division and movement. In support of these functions, the filamentous actin (F-actin) network must participate in the lumen formation of the 3D-reconstitution model at the right time and place with the right organization.^[17] Here, to better understand how the initial lumen of sweat gland placodes is formed in our 3D culture systems, we analyzed proliferation marker Ki67 and cellular motility marker F-actin throughout the overall process, and

also discerned cell death signal markers in the lumen, including those of autophagy and apoptosis, discovering that autophagy participated in the formation of the lumen. To further determine the role of autophagy in the formation of the lumen, we verified the restrictive effect of autophagy inhibitors 3-methyladenine (3MA) on the formation of the lumen, confirming that autophagy rather than apoptosis plays a role in lumen formation of eccrine sweat organoids in 3D-reconstruction models.

Methods

Ethical approval

The patients provided informed consent, and this study was approved by Research Ethics Committee at the Hubei University of Medicine (No.2020-YH-004). The experiments were performed in accordance with the protocols approved by the Institute of Wound Repair and Dermatologic Surgery.

Primary culture of ESGCs

From June to October 2020, non-cauterized and full-thickness skin specimens were obtained from 5 patients undergoing plastic surgery from the Department of Wound Repair and Dermatologic Surgery of Taihe Hospital. The sample individuals are all Han Chinese, including 3 males and 2 females, with an average age of 19.2 ± 3.4 years. The regions include fingers, abdomens, and arms. The samples were stored and transported at 4°C once they were excised, and the storage period was not >8 h when used in subsequent experimental research.

Human ESGCs were obtained as described previously.^[12] Briefly, the human skin specimens were cut into small pieces and then were incubated in 0.2% type II collagenase (Invitrogen 17101015; Invitrogen, Carlsbad, CA, USA) at 37°C for 30 min. After the sweat glands were mechanically isolated using a pipette tip under a light microscope, eccrine sweat glands were picked and planted in a petri dish containing 100 µg/mL pre-coated type IV collagen (Sigma Aldrich, St. Louis, MO, USA). Sweat gland maintenance media consisted of 1:1 Dulbecco's modified Eagle's medium and Ham's F-12 nutrient mixture (Invitrogen 11330032) supplemented with 2% fetal bovine serum (Invitrogen 10099141), 10 ng/mL epidermal growth factor (Invitrogen PHF0311), 1% insulin-transferrin-selenium liquid media supplement (Gibco, Carlsbad, CA, USA), 0.4 µg/mL hydrocortisone (Sigma H4001), 2 ng/mL triiodothyronine (Sigma T6397), 2 mmmol/L GlutaMAX, 100 U/mL penicillin, and 100 µg/mL streptomycin sulfate (Invitrogen 15140122). Media for inhibiting autophagy was replaced with maintenance media with an extra 10 mmmol/L 3MA (Sigma M9281). All procedures were performed under sterile conditions.

Reconstruction of eccrine gland organoids (EGOs) *in vitro*

The isolated ESGCs (2×10^5 per well) were suspended in 500 µL of sweat gland maintenance media and were mixed with 500 µL Matrigel Basement Membrane Matrix (BD (BD, Sparks, MD, USA)) on ice. The mixtures were plated onto six-well plates and were placed into a humidified

incubator at 37°C with 5% CO₂ for 30 min. Two milliliters of pre-warmed maintenance medium were added to the upper layer of the solidified Matrigel. The fresh medium was replaced every 48 h in the first 7 days and every 24 h in the last 7 days. EGO images were acquired at ×10 and ×40 resolution with a charge-coupled device-microscope (Leica, Germany) using a brightfield filter.

Hematoxylin and eosin (H&E) and immunofluorescence staining

The EGOs were washed with cooled phosphate-buffered saline (PBS) for 5 min and were fixed in 4% paraformaldehyde at 4°C for 2 h. After centrifugation at 400 ×g for 15 min, the supernatant was discarded, and the EGOs were embedded in paraffin. For H&E staining, dewaxed 5 μm sections were stained with hematoxylin (Solarbio, Beijing, China) at room temperature (RT) for 3 min, and blue staining was performed by rinsing in tap water, while differentiation was achieved by rinsing in 1% acid ethanol. Counterstaining was performed by rinsing with eosin (Solarbio G1120) for 30 s, and dehydration was performed by sequential washing with 95% ethanol, followed by 100% ethanol. For immunofluorescence staining, samples were sectioned and then air-dried for 2 h. The sections were conventionally dewaxed in xylene, rehydrated through grades of alcohol to PBS. The sections were retrieved and the nonspecific sites were blocked, and the sections were permeabilized with 0.5% Triton X-100 (Beyotime, Shanghai, China) for 30 min followed by blocking in 5% goat serum (Beyotime, Shanghai, China) for 1 h. Primary antibodies were incubated at 4°C overnight. The next day, sections were washed with PBS 3 × 5 min, followed by secondary antibody incubation for 2 h at RT, washed 3 × 10 min with PBS, and then mounted with 4',6-diamidino-2-phenylindole (Beyotime) with fluorescent mounting medium for 1 min. All sections were observed under the fluorescent microscope (Leica) under the corresponding optical conditions. The immunofluorescence primary antibodies used in the article include Ki67 (Abcam ab92742, 1:500; Abcam, Cambridge, MA, UK) and LC3B from Cell Signaling Technology (cell Signaling Technology, MA, USA). F-actin signal Actin-Tracker Red-555 was purchased from Beyotime (C2203S), and the apoptotic signal was detected using the One Step TUNEL Apoptosis Assay Kit (C0186) according to the respective manufacturer's instructions.

Western blot

The excess medium was removed at different detection time points, and EGOs were washed and recycled with cell recovery solution (354253; Corning, NY, USA) according to the gel solution ratio (1:1, v/v). After the gel components were completely dissolved, the mixture was transferred into a tube for centrifugation at 400 ×g for 10 min. The pelleted EGOs were resuspended in 1 × PBS, and centrifugation was repeated as previously described. The samples were lysed with cell lysate buffer, and sodium dodecyl sulphate-polyacrylamide gel electrophoresis was performed with the gradient gel. A semi-dry transfer apparatus (Bio-rad, Hercules, CA, USA) was used to

transfer gel protein onto polyvinylidene fluoride (PVDF) membranes (88518; Millipore, Billerica, MA, USA) under 24 V for 50 min. The transferred membranes were blocked in 5% skim milk dissolved in Tris-buffered saline with 0.1% Tween (TBS-T) for 30 min and then washed twice. Subsequently, PVDF membranes were incubated with primary antibody for 2 h. After three 10 min washes with TBS-T, the membranes were incubated with the secondary antibody for 1 h and were sequentially washed in TBS-T three times. Finally, the PVDF membranes were exposed by incubating with an enhanced chemiluminescence detection kit (Millipore WBKLS0500) for the proper amount of time and developed in a processing machine (Koda, Tokyo, Japan) for signal detection. The Western blots assays were performed more than three times with the representative results shown in the [Figure 2C and 3C]. The corresponding antibodies are as follows: Ki67 (Invitrogen SP6, 1:1000), F-actin (Abcam ab130935, 1:500), LC3B (CST 3868T, 1:1000), PARP (CST 9542, 1:1000), cleaved caspase-3 (CST 9664 s, 1:1000), and loading control glyceraldehyde 3-phosphate dehydrogenase GAPDH (Abcam ab181602, 1:1000).

Statistical analysis

Statistical significance was determined using one-way analysis of variance (ANOVA) for comparisons between two groups or among multiple groups using GraphPad Prism, version 8.0 (GraphPad Software, San Diego, CA, USA). The results were represented as the mean ± standard deviation from independent experiments, and a *P* value < 0.05 was considered significant.

Results

EGOs developed from the initial solid structure to the final luminal structure

Organoids are originally established from epithelial stem cells from multiple adult tissues, simulating the morphological development process of their respective origin tissues. In our 3D-reconstruction models, we tracked the cells resuspended in the culture medium and observed the appearance of EGOs and the process of lumen formation. Brightfield, visual field, and H&E staining results showed that the single cells divided and proliferated from day 0 to day 4 and continued to self-multiply or migrate to each other to form multicellular EGOs [Figure 1A and B]. When the cells underwent sustained proliferation and differentiation from day 4 to day 8, we observed that the EGOs were spherical, and the spheroid volume was obviously increased and spatially independent to other EGOs [Figure 1A and B]. The total number of EGO cells similarly doubled at day 8 based on the cross-sectional cell nuclear count results [Figure 1C]. Notably, the internal cells in individual EGOs began to separate from the surrounding cells, and our H&E staining results showed a portion of the rudimentary formation of the lumen structure with a cellular gap at day 6 [Figure 1B]. In the later 3D-reconstruction model phase from day 8 to day 14, the total number of cells in each EGO did not change significantly, as the volume of the EGO sphere increased

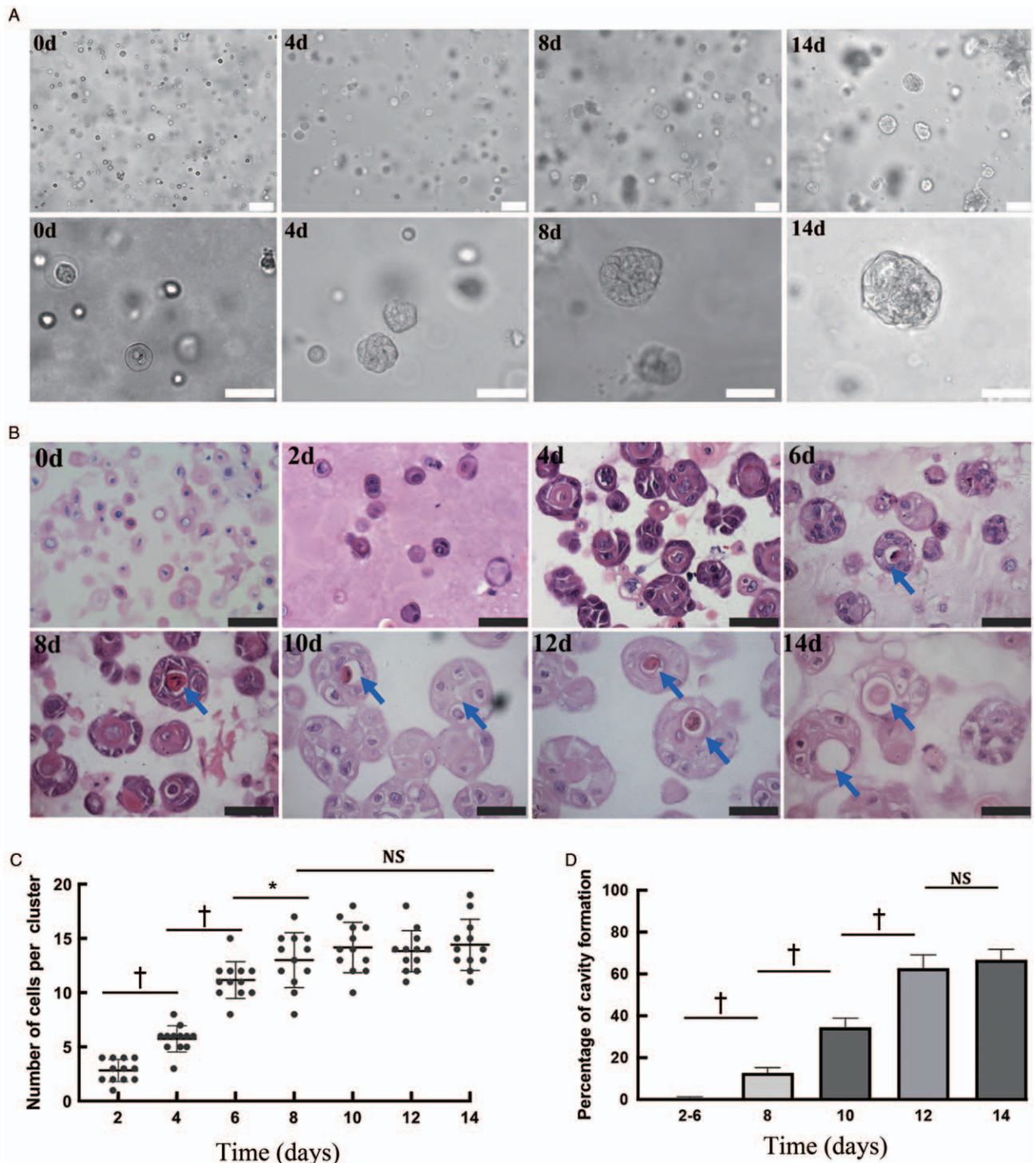


Figure 1: Morphological changes in 3D-reconstructed eccrine glands at different time points. (A) Formation of EGOs in the brightfield view of 3D-reconstructed eccrine glands cells at days 0, 4, 8, and 14; top: original magnification 10 × and bottom: original magnification 40 × magnified vision. (B) Lumen formation progress of EGOs by HE staining of 3D-reconstructed eccrine gland cells. The blue arrows indicate the lumen inside the EGOs. (C) Representative blots of the total number of cells per EGO (n = 12) cross-section. (D) The percentage of the lumen formed in EGOs at different time points. Representative images and graphics results from three independent experiments of eccrine sweat gland 3D-reconstruction, mean ± SD. NS: not statistically significant; P > 0.05, *P < 0.01, †P < 0.0001; white and black scale bars, 50 μm. EGO: Eccrine gland organoid; H&E: Hematoxylin and eosin.

slightly, and the lumen’s tubular cavity shape was more recognizable. With the gradual metabolic disintegration of internal cells in the vacuoles followed by absorption, it was obvious that a hollow shape similar to a lumen exists in most EGOs, which increases the proportion of vacuoles [Figure 1B].

Formation of EGOs depends on cell proliferation and polarization-driven membrane separation

To further verify that the antigen expression of EGOs at different time points is related to proliferation, we performed immunofluorescence staining of the relevant

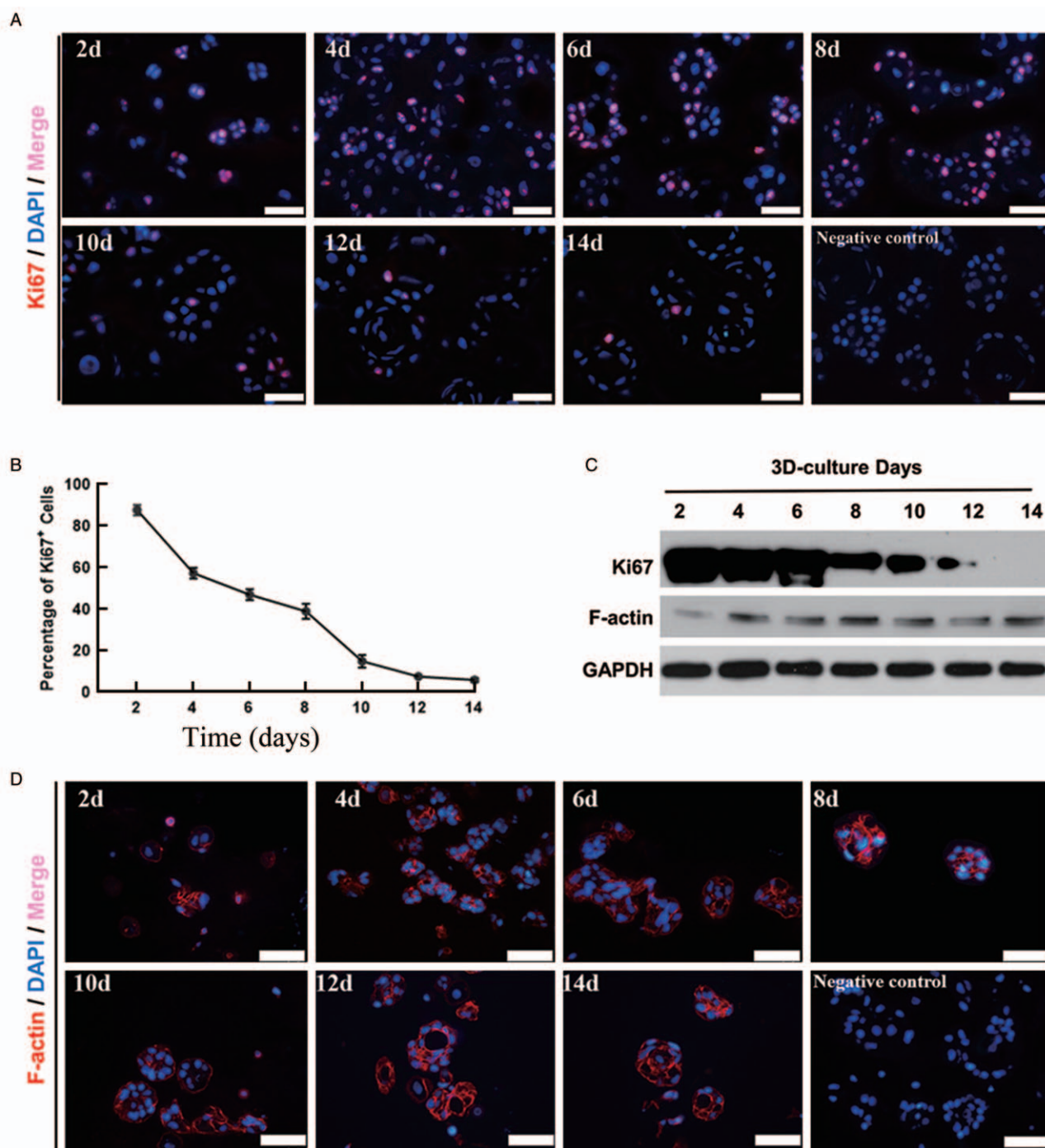


Figure 2: Proliferation and epithelial cell polarization of 3D-reconstructed eccrine glands cells determined the morphological changes. (A) Immunofluorescence analysis of cell proliferation marker Ki67 and (B) quantification of the positive rate of Ki67 expression in total sweat gland cells ($n = 50$) at different time points. (C) Western blot analysis showed expression of Ki67, F-actin, and GAPDH (loading control) at different 3D-reconstructed days in three independent experiments. (D) Immunofluorescence results of cell polarization marker F-actin expression at different time points. DAPI (blue) stain nuclei. Negative control, the day 14 samples were incubated with PBS instead of primary antibodies during immunofluorescence reactions. Representative image of the observations in EGOs derived from three independent experiments. Scale bars, 50 μ m. DAPI: Diamidino-2-phenylindole; EGO: Eccrine gland organoid; F-actin: Filamentous actin; PBS: Phosphate-buffered saline.

antigen expressing Ki67. The results showed that Ki67 expression was higher in the early and mid-term stages of the 3D remodeling process of eccrine gland cells from day 0 to day 8, as the volume of change was inversely proportional [Figure 2A]. The results of our analyses on the positive cells found that the positive rate gradually decreased with the culture time [Figure 2B], and the

Western blot results also proved that the expression of Ki67 in the EGO total protein was significantly reduced [Figure 2C]. For an illustration of the epithelial cell-driven polarization in the participating EGOs formation, the key factor in the process of cluster morphology changes, F-actin, was also analyzed to study cell polarization movement protein expression. Although there was little

difference in the F-actin expression level of the Western blot assay during the 14-day culture cycle, the results of the immunofluorescence experiment showed that F-actin was significantly expressed in the whole cell cluster, specifically on the formed spherical surface before the EGO lumen formation from day 2 to day 4. After day 6, F-actin accumulated on the surface of the inner membrane of EGOs, and we clearly observed that the nuclei of the peripheral cells of the EGOs were gradually flattened with the spherical body, causing the internal cavity to further expand to form a structure similar to a lumen [Figure 2C and D]. These results indicate that cell polarization movement was involved in the separation of the inner cells of early EGOs.

Autophagy, not apoptosis, induces lumen formation

We questioned whether cell death accompanied by metabolic decomposition initiates the formation of EGO lumens. Therefore, two cellular death modes, autophagy and apoptosis, were tested separately in our 3D-reconstruction time points. We performed immunohistochemistry on paraffin sections prepared from day 2 to day 14 and found a positive LC3B signal in EGO internal cells where the TUNEL signal was negative. In our Western blot assay, the high expression of cell autophagy marker LC3B together with the absence of signaling of apoptotic cells (cleaved PARP and cleaved Caspase-3) within EGOs demonstrated that autophagy was identified as the main cell death mode mechanism [Figure 3A–C]. The increased autophagy ratio was detected from day 8 to day 14, and it was essentially the same as the time it took for EGOs to form lumens [Figure 3D]. During this time period, the proportion of apoptotic EGOs failed to increase significantly, indicating that apoptosis was not involved in the process of EGO lumen formation. Subsequently, to further verify the important role of internal cell autophagy in the formation of lumens in EGOs, we added autophagy inhibitor 3-MA to the initial Matrigel and conditioned medium to detect whether it could inhibit the formation of lumens in a limited manner. The results of immunofluorescence staining showed that LC3B-positive cells decreased after treatment with 3-MA of a 3D culture at day 14 [Figure 4A]. A recognizable morphological change was also observed by measuring EGOs external diameter *D* and inner lumen diameter *L* [Figure 4B]. Although 3-MA has almost no effect on the average outer diameter of EGOs, an increase in lumen diameter was observed without adding inhibitor 3-MA [Figure 4C], confirming that autophagy of cells plays an important role in the formation of lumen structures in EGOs.

Discussion

Establishing sweat gland cell 3D-remodeling in Matrigel and exploring the mechanism of sweat gland lumen formation are essential for a better understanding of the basic process of sweat gland development and the relationship between lumen functional differentiation and sequential structure *in vivo*.^[6] In this work, we have described the temporal progression of the biological events such as cell migration, proliferation, and polarization that

contribute to the morphogenesis of a lumen structure *in vitro* and have confirmed that autophagy is involved in the clearance of inner cells of EGOs during lumen formation [Figure 4D]. Before the lumen was formed, the sweat gland cell monomer divided and proliferated to form a multicellular structure, and these multimers migrated to the border to fuse with each other, thereby forming an EGO. Since the cells inside the EGOs cannot access the nutrients of the Matrigel and conditioned medium, the programmed cell death caused by abnormal metabolism could create a cavity at the center of each EGO. With the further polarization movement of the living cells in the inner layer, a circular or spherical vacuole structure similar to a glandular lumen was formed in the center of the cluster. Our previous studies have shown that a structure similar to the sweat gland lumen could be observed when subcutaneously cultured in the groin of nude mice with 3D Matrigel.^[18] Our studies also showed similar expression and distribution of multiple antigens such as S100P, S100A2, alpha-smooth muscle actin, and nerve fiber markers protein gene product 9.5 (PGP 9.5), which confirmed that the lumen formed in the process of culturing sweat gland cells corresponds to the construction of the early sweat gland lumen in the body.^[16,19] Therefore, we can infer that the lumen structure in our EGOs is similar to the primary structure of sweat gland ducts in body development.

Due to specific interactions between the extracellular matrix (ECM) and neighboring cells, the inner cells of EGOs underwent a distinct fate decided by a particular location. Anoikis, a form of apoptosis caused by inappropriate cell/ECM interactions, has been reported in the formation of the lumen during the development of various secretory glands such as mammary and salivary glands.^[20,21] However, our TUNEL staining and immunohistochemical staining of Caspase-3 results (data not shown) do not show an evident apoptotic signal generating internal EGOs during the entire 14 days. The autophagy signal of cells in the lumen suggests that the formation of the lumen may not be directly related to the apoptosis of internal cells. It is worth noting that Debnath *et al*.^[22] recently proved that the inhibition of apoptosis through the ectopic expression of the anti-apoptotic protein Bcl-2 cannot terminate the formation of the lumen, which indicated that the induction of autophagy contributed to the survival of epithelial cells during oxygen-deficient environment in the 3D hollow formation. In addition, multiple research results have shown that autophagy protects cells exposed to various forms of stress, including nutrient deprivation, growth factor regression, endoplasmic reticulum stress, and ischemia.^[23–25] In the later stage of our 3D-reconstruction system culture, each EGO is composed of multiple layers of cells (similar to the two layers of the sweat gland lumen in the body),^[2] and the formation of hollowing cells was more common in monolayer cell columns. The hollowing form was usually seen in the early stage of formation of the lumen of blood vessels and the formation of the intestinal lumen of zebrafish, and these developmental processes were generally not accompanied by cell death.^[26,27] In our studies, inner cell autophagy participated in the formation of the lumen, and other reports also indicated that the formation

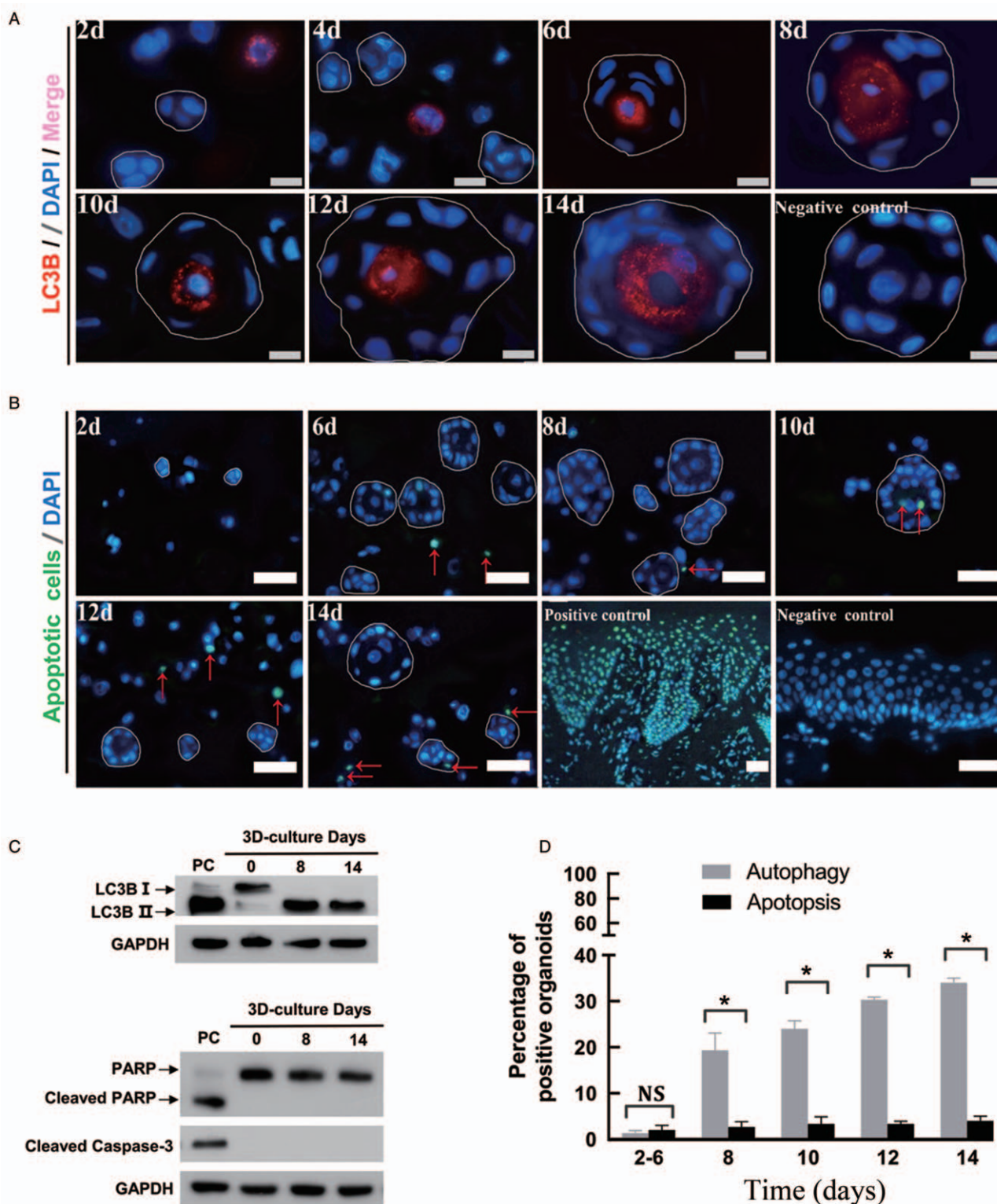


Figure 3: Autophagy, not apoptosis, causes the formation of EGO lumens. (A) Immunofluorescence analysis of the expression of the LC3B cell autophagy marker at different time points. Each white circle is independently marked to represent an integrated EGO. Gray scale bars, 20 μm. (B) The TUNEL assay was analyzed by staining the apoptotic index cell in the field. The red arrows indicate positive cells. The positive control comes from the positive standard sample by the reagent kit. White scale bars, 50 μm. (C) Western blot analysis showing the expression of LC3B (autophagy marker), PARP, and cleaved caspase-3 (apoptosis markers) in 3D-reconstructed EGOs at days 0, 8, and 14. PC, positive control, induce by 10 nmol rapamycin for autophagy and 200 ng/mL TNF-related apoptosis-inducing ligand (TRAIL) for apoptosis respectively at 3D-reconstructed day 0. (D) Quantitation of the proportion of autophagic and apoptotic positive cell organoids in total EGOs at different time points. The values shown are the mean ± SD from three different experiments. NS: not statistically significant; $P > 0.05$, * $P < 0.001$; EGO: Eccrine gland organoid.

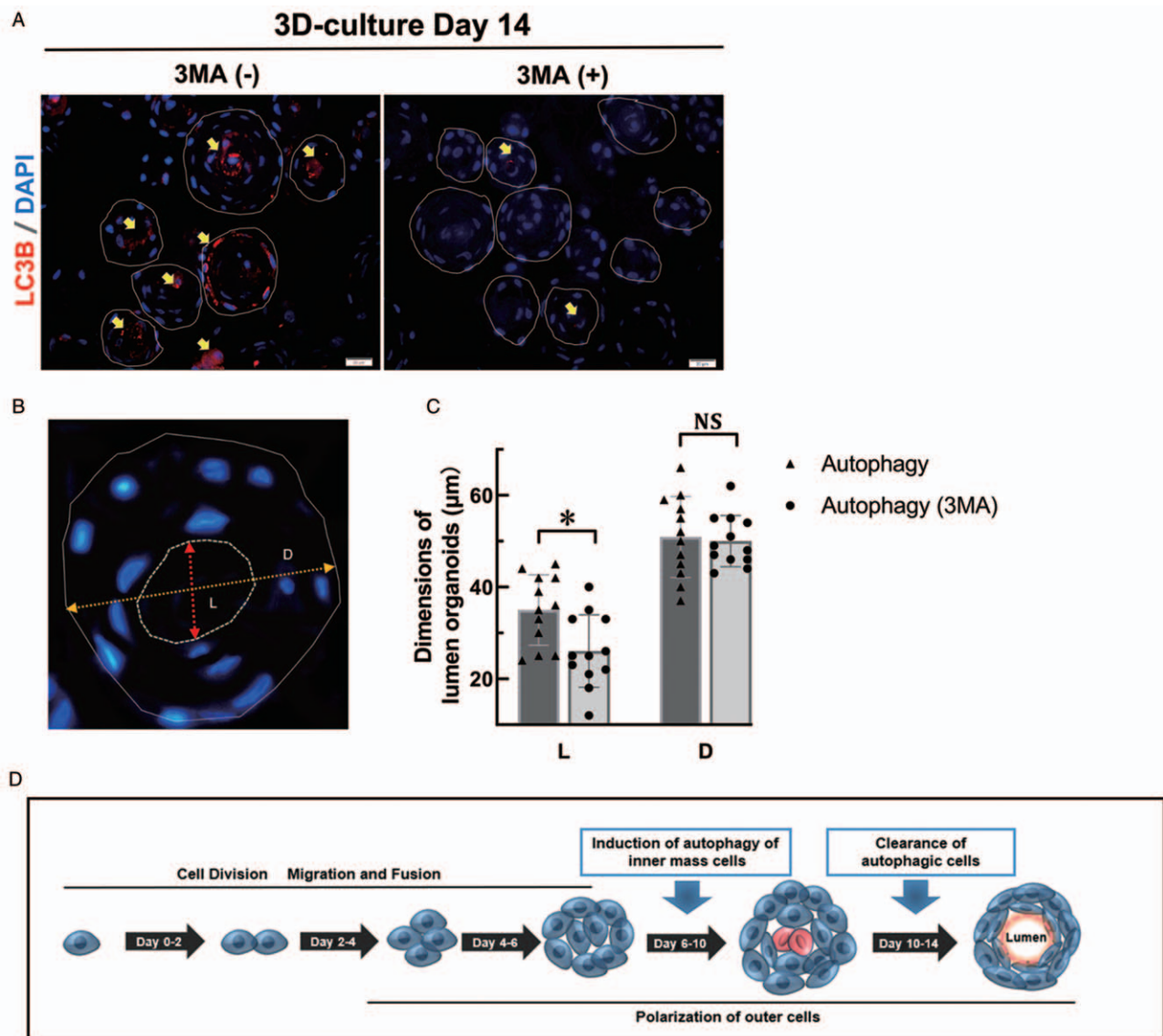


Figure 4: Autophagy inhibitor 3MA can limit the formation of sweat gland organoid cavities. (A) Immunofluorescence analysis of the expression of LC3B at day 14 treated with 10 mmol/L autophagy inhibitor 3MA. Each white circle is independently marked to represent an integrated sweat gland organoid. The yellow arrows indicate the expression of the autophagy marker LC3B in the lumen. Scale bars, 20 μm. (B) Reference pattern of length was measured across an EGO as indicated by the yellow arrow, D, diameter, and red arrow, L, lumen. (C) Quantification of the average size of diameter and inter lumen of EGOs ($n = 12$) treated with or without autophagy inhibitor 3MA. The values shown are mean \pm SD from three different experiments. NS (not statistically significant), $P > 0.05$, $*P < 0.001$. (D) Schematic representation of the lumen formation during 3D-reconstructed eccrine glands cells *in vitro*. Autophagy of inner cells synergized with the polarized movement of outer cells to promote the lumen formation of EGOs. 3MA: 3-methyladenine; EGO: Eccrine gland organoid.

of the glandular lumen is mostly accompanied by apoptosis or autophagy. In summary, the polarized and flat outer layer of cells surrounded the cells in the inner center layer by layer, resulting in insufficient nutrition of the inner cells and further autophagy.

Our 3D-reconstruction lumen formation model cannot spatiotemporally imitate the luminal form of sweat glands in the body as placode invagination, and the results of our immunofluorescence experiment to identify LC3B failed to stain the autophagy signal around the basal cells in the embryonic base from mouse sweat gland duct formation period of E15 to P5 (data not shown). Nevertheless, Diao *et al*^[28] reported that sweat gland organoids that were formed from epithelial cells from the dermal sweat glands

of adult mouse paw pads embedded in Matrigel can effectively restore the ductal morphology and sweat secretion function of sweat glands after transplantation into the paws of mice with damaged sweat glands. On the other hand, in our experimental system, the autophagy inhibitor 3-MA can effectively inhibit the occurrence of autophagy in the lumen and make the inner diameter of the lumen smaller, showing that autophagy is directly related to the formation of the lumen. These results indicate that the 3D model has certain significance.

Funding

This manuscript was supported in part by the grants from the National Natural Science Foundation of China (Nos.

82172231, 81772102) and the Taihe Foundation No. 2021JJXM060.

Conflicts of interest

None.

References

- Cui CY, Schlessinger D. Eccrine sweat gland development and sweat secretion. *Exp Dermatol* 2015;24:644–650. doi: 10.1111/exd.12773.
- Lu C, Fuchs E. Sweat gland progenitors in development, homeostasis, and wound repair. *Cold Spring Harb Perspect Med* 2014;4:a015222. doi: 10.1101/cshperspect.a015222.
- Mailleux AA, Overholtzer M, Brugge JS. Lumen formation during mammary epithelial morphogenesis: insights from in vitro and in vivo models. *Cell Cycle* 2008;7:57–62. doi: 10.4161/cc.7.1.5150.
- Patel N, Sharpe PT, Miletich I. Coordination of epithelial branching and salivary gland lumen formation by Wnt and FGF signals. *Dev Biol* 2011;358:156–167. doi: 10.1016/j.ydbio.2011.07.023.
- Hogan BLM, Kolodziej PA. Organogenesis: molecular mechanisms of tubulogenesis. *Nat Rev Genet* 2002;3:513–523. doi: 10.1038/nrg840.
- Clevers H. Modeling development and disease with organoids. *Cell* 2016;165:1586–1597. doi: 10.1016/j.cell.2016.05.082.
- Nguyen-Ngoc KV, Shamir ER, Huebner RJ, Beck JN, Cheung KJ, Ewald AJ. 3D culture assays of murine mammary branching morphogenesis and epithelial invasion. *Methods Mol Biol* 2015; 1189:135–162. doi: 10.1007/978-1-4939-1164-6_10.
- Bakhti M, Scheibner K, Tritschler S, Bastidas-Ponce A, Tarquis-Medina M, Theis FJ, *et al.* Establishment of a high-resolution 3D modeling system for studying pancreatic epithelial cell biology in vitro. *Mol Metab* 2019;30:16–29. doi: 10.1016/j.molmet.2019.09.005.
- Pradhan S, Liu C, Zhang C, Jia X, Farach-Carson MC, Witt RL. Lumen formation in three-dimensional cultures of salivary acinar cells. *Otolaryngol Head Neck Surg* 2010;142:191–195. doi: 10.1016/j.otohns.2009.10.039.
- Xiao S, Zhang Y. Establishment of long-term serum-free culture for lacrimal gland stem cells aiming at lacrimal gland repair. *Stem Cell Res Ther* 2020;11:20. doi: 10.1186/s13287-019-1541-1.
- Blasky AJ, Mangan A, Prekeris R. Polarized protein transport and lumen formation during epithelial tissue morphogenesis. *Annu Rev Cell Dev Biol* 2015;31:575–591. doi: 10.1146/annurev-cellbio-100814-125323.
- Li H, Chen L, Zhang M, Tang S, Fu X. Three-dimensional culture and identification of human eccrine sweat glands in matrigel basement membrane matrix. *Cell Tissue Res* 2013;354:897–902. doi: 10.1007/s00441-013-1718-3.
- Li H, Zhang M, Chen L, Zhang B, Zhang C. Expression of S100A2 and S100P in human eccrine sweat glands and their application in differentiating secretory coil-like from duct-like structures in the 3D reconstituted eccrine sweat spheroids. *J Mol Histol* 2017;48:219–223. doi: 10.1007/s10735-017-9721-8.
- Li X, Li H, Zhang M, Chen L, Zhang B. Cell proliferation and differentiation during the three dimensional reconstitution of eccrine sweat glands. *J Mol Histol* 2017;48:113–120. doi: 10.1007/s10735-017-9710-y.
- Zhang M, Li H, Chen L, Fang S, Xie S, Lin C. Three-dimensional reconstructed eccrine sweat glands with vascularization and cholinergic and adrenergic innervation. *J Mol Histol* 2018;49: 339–345. doi: 10.1007/s10735-018-9773-4.
- Zhang M, Li H, Xie S, Chen L. Time course of differentiation of different cell types in 3D-reconstructed eccrine sweat glands. *J Mol Histol* 2018;49:567–575. doi: 10.1007/s10735-018-9795-y.
- Kadzik RS, Homa KE, Kovar DR. F-actin cytoskeleton network self-organization through competition and cooperation. *Annu Rev Cell Dev Biol* 2020;36:35–60. doi: 10.1146/annurev-cellbio-032320-094706.
- Li H, Zhang M, Chen L, Li X, Zhang B. Human eccrine sweat gland cells reconstitute polarized spheroids when subcutaneously implanted with Matrigel in nude mice. *J Mol Histol* 2016;47:485–490. doi: 10.1007/s10735-016-9690-3.
- Ouyang Z, Li HH, Zhang MJ, Xie ST, Cheng LHH. Differential innervation of secretory coils and ducts in human eccrine sweat glands. *Chin Med J (Engl)* 2018;131:1964–1968. doi: 10.4103/0366-6999.238142.
- Gilmore AP. Anoikis Cell Death Differ 2005;12:1473–1477. doi: 10.1038/sj.cdd.4401723.
- Fung C, Lock R, Gao S, Salas E, Debnath J. Induction of autophagy during extracellular matrix detachment promotes cell survival. *Mol Biol Cell* 2008;19:797–806. doi: 10.1091/mbc.e07-10-1092.
- Debnath J. Detachment-induced autophagy during anoikis and lumen formation in epithelial acini. *Autophagy* 2008;4:351–353. doi: 10.4161/auto.5523.
- Satyavarapu EM, Das R, Mandal C, Mukhopadhyay A, Mandal C. Autophagy-independent induction of LC3B through oxidative stress reveals its non-canonical role in anoikis of ovarian cancer cells. *Cell Death Dis* 2018;9:934. doi: 10.1038/s41419-018-0989-8.
- Whelan KA, Reginato MJ. Surviving without oxygen: hypoxia regulation of mammary morphogenesis and anoikis. *Cell Cycle* 2011;10:2287–2294. doi: 10.4161/cc.10.14.16532.
- Chen N, Eritja N, Lock R, Debnath J. Autophagy restricts proliferation driven by oncogenic phosphatidylinositol 3-kinase in three-dimensional culture. *Oncogene* 2013;32:2543–2554. doi: 10.1038/onc.2012.277.
- Sacharidou A, Stratman AN, Davis GE. Molecular mechanisms controlling vascular lumen formation in three-dimensional extracellular matrices. *Cells Tissues Organs* 2012;195:122–143. doi: 10.1159/000331410.
- Sigurbjornsdottir S, Mathew R, Leptin M. Molecular mechanisms of de novo lumen formation. *Nat Rev Mol Cell Biol* 2014;15:665–676. doi: 10.1038/nrm3871.
- Diao J, Liu J, Wang S, Chang M, Wang X, Guo B, *et al.* Sweat gland organoids contribute to cutaneous wound healing and sweat gland regeneration. *Cell Death Dis* 2019;10:238. doi: 10.1038/s41419-019-1485-5.

How to cite this article: Du L, Zhang L, Zhao J, Chen Z, Liu X, Cao M, You L, Zhang Y, Fu X, Li H. Autophagy, not apoptosis, plays a role in lumen formation of eccrine gland organoids. *Chin Med J* 2022;135:324–332. doi: 10.1097/CM9.0000000000001936